Association of Peritoneal Dialysis Effluent Interleukin-17 with Peritoneal Functional Decline and Clinical Significance: A Prospective Cohort Study

Authors

Lejia Song, Lu Li, Guang Chen, Qiufeng Wang, Qingqing Rao, Huaina Dou, Li Zhang, Pei Zhang

Correspondence

zhangpei@ahmu.edu.cn (P. Zhang)

Graphical Abstract

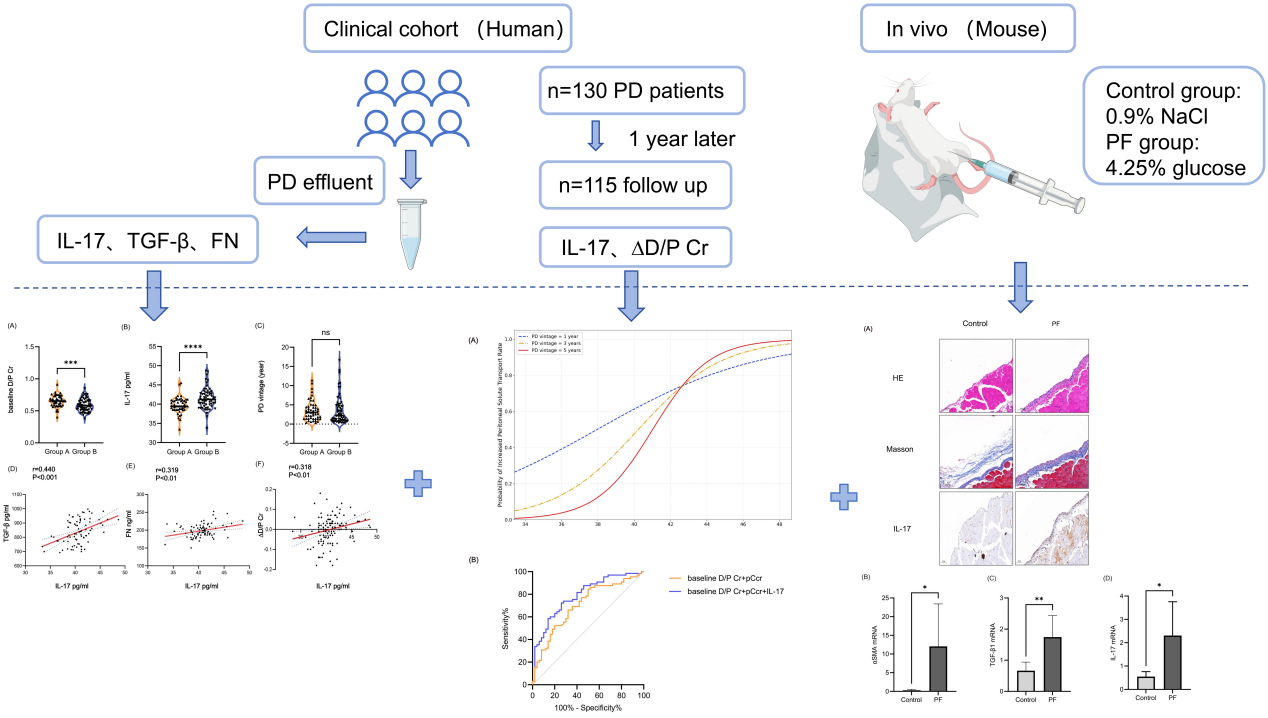

https://doi.org/10.71321/g94y8w65

Research Article

Life Conflux

Association of Peritoneal Dialysis Effluent Interleukin-17 with Peritoneal Functional Decline and Clinical Significance: A Prospective Cohort Study

Lejia Song [1,2†], Lu Li [1,2†], Guang Chen [1,2], Qiufeng Wang [1], Qingqing Rao [1,2], Huaina Dou [2], Li Zhang [2], Pei Zhang [1,2*]

Received: 2026-02-19 | Accepted: 2026-04-15 | Published online: 2026-05-26

Abstract

Background: Long-term peritoneal dialysis (PD) frequently induces chronic peritoneal inflammation, fibrosis, and increased peritoneal solute transport rate (PSTR). This study assessed whether effluent interleukin-17 (IL-17) predicts increased PSTR and relates to peritoneal fibrosis.

Methods: This prospective cohort enrolled 130 PD patients, of whom 115 completed 1-year follow-up. Effluent IL-17, transforming growth factor-β (TGF-β), and fibronectin (FN) were measured by enzyme-linked immunosorbent assay (ELISA). Peritoneal function was assessed by dialysate-to-plasma creatinine ratio (D/P Cr) at baseline and 1 year. We used correlation analysis, multivariable regression, interaction analysis, and Receiver operating characteristic (ROC) analysis to evaluate the predictive value of effluent IL-17 for increased PSTR. A mouse peritoneal fibrosis model was used to evaluate local IL-17 expression by immunohistochemistry and real-time quantitative PCR (RT-qPCR).

Results: Effluent IL-17 was higher in patients with increased PSTR and correlated positively with TGF-β, FN, and ΔD/P Cr. Multivariable analysis showed that IL-17 independently predicted 1-year D/P Cr after adjustment for baseline D/P Cr and clinical covariates. PD vintage significantly modified the association between IL-17 and increased PSTR. Adding IL-17 to baseline D/P Cr and peritoneal creatinine clearance improved prediction of increased PSTR, with the AUC increasing from 0.705 to 0.789. Furthermore, immunohistochemical and qPCR results showed that IL-17 expression was elevated in fibrotic peritoneal tissues of PF mice compared with control mice.

Conclusion: Effluent IL-17 is associated with peritoneal fibrosis and longitudinal PSTR increase, supporting its potential as a noninvasive biomarker for early risk stratification in PD patients.

Keywords: Peritoneal dialysis; Peritoneal fibrosis; Peritoneal function; Biomarker; IL-17

Introduction

Peritoneal dialysis (PD) is a vital treatment option for end-stage renal disease (ESRD) worldwide, as evidenced by its simplicity, cost-effectiveness, and ability to preserve residual renal function [1]. The efficacy of this therapeutic modality relies heavily upon maintaining the architectural and physiological integrity of the peritoneal membrane. However, chronic inflammation and peritoneal injury are induced by chronic exposure to bioincompatible dialysate (characterized by hypertonicity, high glucose, and acidity). These pathological changes include mesothelial cell denudation, neovascularization, and excessive extracellular matrix deposition, eventually progressing to submesothelial fibrosis [2]. Such structural remodelling compromises vascular permeability and disrupts transport kinetics, driving ultrafiltration failure (UFF) and, ultimately, technique failure [3].The peritoneal equilibration test (PET) remains the clinical standard for evaluating peritoneal function through the quantification of solute transport and ultrafiltration capacity. This assessment relies on measuring the dialysate-to-plasma creatinine ratio (D/P Cr), the 4-hour to 0-hour dialysate glucose ratio (D/D0 glucose), and the 4-hour ultrafiltration volume (4 h UF) [4]. A faster peritoneal solute transport rate (PSTR) is predictive of adverse clinical outcomes. Specifically, an increase of 0.1 units in D/P Cr is associated with a significantly elevated risk of technique failure, hospitalization, and all-cause mortality [5-6]. However, while PET effectively reflects current transport characteristics, it lacks the sensitivity required for the early detection of peritoneal function decline.

While specific effluent biomarkers have been identified, their clinical applications remain limited. Interleukin-6 (IL-6) is correlated with solute transport, inflammation, and fibrosis. However, its diagnostic specificity is compromised by interference from systemic inflammation and interindividual variability [7]. Similarly, cancer antigen 125 (CA125) has been recognized as a biomarker for mesothelial cell mass. Nevertheless, CA125

1 Department of Nephropathy, The First Affiliated Hospital of Anhui Medical University, Hefei, China.

2 Anhui Medical University, Hefei, China.

† These authors have contributed equally to this work.

* Corresponding Author.

shows limited prognostic value for adverse outcomes, such as peritonitis or ultrafiltration failure, when used as a single marker [8]. Therefore, the identification of highly specific biomarkers to accurately characterize peritoneal pathological mechanisms remains a critical research priority.

Interleukin-17A (IL-17) is the signature cytokine of the T helper 17 (Th17) lineage. It plays a critical role in regulating inflammation and angiogenesis in autoimmune pathologies, such as multiple sclerosis and rheumatoid arthritis [9]. Mechanistically, IL-17 orchestrates a continuous inflammatory response by enhancing Th17 cell differentiation through the IL-6/TGF-β/RORγt (Interleukin-6/ transforming growth factor β/ retinoic acid-related orphan receptor gamma t) axis and recruiting immune cells via CCL20-dependent chemotaxis [10-11]. While IL-17 levels are negligible in the peritoneum of healthy individuals, this cytokine is significantly upregulated in the peritoneum of patients receiving PD. These elevated levels originate primarily from infiltrating Th17 and γδ T cells [12]. Moreover, accumulating evidence suggests that IL-17 promotes fibrosis across various organ systems. For example, it promotes myocardial fibrosis by activating cardiac fibroblasts, induces pulmonary fibrosis through mitochondrial dysfunction-mediated epithelial apoptosis, and exacerbates liver fibrosis by enhancing TGF-β receptor signalling [13-15]. In hypertensive nephropathy and IgA nephropathy, studies have shown that IL-17 activates downstream signalling cascades, notably NF-κB, to induce the release of inflammatory mediators and aberrant extracellular matrix deposition, consequently driving the progression of renal fibrosis [16-17]. However, research concerning the expression of IL-17 in peritoneal tissue and its correlation with impaired peritoneal function remains limited.

Therefore, in this study, the expression of IL-17 in PD effluent was prospectively evaluated, and its ability to predict longitudinal peritoneal function decline was evaluated, with the goal of identifying a novel noninvasive biomarker for early risk stratification.

Methods

Study Design and Population

This prospective cohort study included 130 patients who received regular PD follow-up at the Department of Nephrology, the First Affiliated Hospital of Anhui Medical University, between September 2023 and September 2025. The follow-up duration was 1 year. This research was approved by the Ethics Committee of the First Affiliated Hospital of Anhui Medical University (approval number: PJ 2025-08-97).

Eligible patients were aged between 18 and 80 years, on stable peritoneal dialysis replacement therapy (PD vintage ≥ 3 months) using only commercially available peritoneal dialysis solutions with 1.5% or 2.5% glucose, and had a stable PD regimen (no adjustments for at least 1 month). Exclusion criteria included peritonitis within the past month, autoimmune diseases (e.g., lupus nephritis, rheumatoid arthritis, Sjögren's syndrome, and chronic lymphocytic thyroiditis), infections (e.g., hepatitis B virus, hepatitis C virus, and syphilis), malignant or benign tumors, and use of antibiotics or hormones at the time of sample collection.

All animal procedures were approved by the Animal Ethics Committee of Anhui Medical University (Approval Number: LLSC20241406).

Male C57BL/6 mice (20–24 g, n = 12) were randomly allocated into two groups (control group n = 6, PF group n= 6). To establish a peritoneal fibrosis (PF) model, mice in the experimental group received daily intraperitoneal injections of 2 mL of 4.25% glucose-based dialysis solution for 28 consecutive days. The control group received an equal volume of isotonic saline (0.9% NaCl) following the same schedule.

Data Collection and Variables

General clinical data included the following: (1) demographic characteristics, such as age, sex, height, weight, and body mass index (BMI); (2) PD vintage, defined as the time from PD initiation to study enrolment (years); (3) comorbidities such as diabetes mellitus, hypertension, and cardiovascular disease; and (4) laboratory examinations, including routine biochemical parameters (renal function, blood urea nitrogen (BUN), serum creatinine (Scr), and parathyroid hormone (PTH)), electrolytes (serum calcium and serum phosphate (P)), nutritional indicators (serum albumin [Alb] and haemoglobin [Hb]), lipid metabolism parameters (total cholesterol [TC] and triglyceride [TG]), inflammatory markers (neutrophil count [NE], lymphocyte count [LYM], monocyte count [MONO], and C-reactive protein [CRP]), and corrected serum calcium concentration calculated as: corrected serum calcium (mmol/L) = serum calcium + 0.02 × (40 − Alb [g/L]).

Cardiac indices included left ventricular ejection fraction (EF), left atrial diameter (LA), left ventricular diameter (LVD), and left ventricular posterior wall thickness (LVPWD).

Peritoneal Function Measurement

On the night before the PET, patients were required to retain peritoneal dialysis fluid for 8–12 hours. On the test day morning, after emptying the bladder and bowels, patients assumed a standing position, and the existing PD fluid was completely drained from the peritoneal cavity within 20 minutes. Subsequently, 2 L of 2.5% glucose PD solution was rapidly infused into the peritoneal cavity within 10 minutes, with patients turning from side to side after each 400 mL administration. Upon completion of infusion, the dialysis tubing was clamped, and the PD fluid was retained in the peritoneal cavity for 4 hours. First, original PD fluid was collected immediately (0 minutes) after complete infusion to obtain a 0-hour PD fluid sample. At exactly 2 hours of dwell time, venous blood and PD effluent samples were collected. After maintaining the dialysis position for precisely 4 hours, patients switched to a seated or standing posture, and the PD fluid in the peritoneal cavity was completely drained into a collection bag within 20 minutes. Following drainage, the total volume of effluent was measured and recorded. Subsequently, additional PD effluent samples were collected from the drainage bag [4].

The following parameters were calculated:

Dialysate-to-plasma creatinine ratio (D/P Cr) = dialysate creatinine (4 h) / plasma creatinine (2 h)

Dialysate glucose ratio (D/D0 glucose) = dialysate glucose (4 h) / dialysate glucose (0 h)

At 12 months (±1 month) after baseline, peritoneal function parameters D/P Cr and D/D0 glucose were evaluated again.

Definitions:

ΔD/P Cr = D/P Cr 1 year later − baseline D/P Cr

ΔD/D0 glucose = D/D0 glucose 1 year later − baseline D/D0

glucose
Faster PSTR was defined as ΔD/P Cr > 0 at 1-year follow-up.

Biomarker Detection
Peritoneal effluent sample collection: After rigorous application of the inclusion and exclusion criteria, 10 mL of 4-hour peritoneal dialysis effluent was collected from the study subjects. The samples were aliquoted and balanced in a laboratory centrifuge. The centrifuge was set to 3,600 RPM and run for 10 minutes. The resulting precipitate was removed, and the supernatant solution was collected and aliquoted into EP tubes (1 mL per tube). To avoid repeated freeze-thaw cycles, aliquots were immediately placed in a -80 °C freezer to await analysis.
Enzyme-linked immunosorbent assay (ELISA) kits were provided by MeiKe. The supernatant stored at −80 °C was thawed at room temperature, then vortexed and centrifuged again. All experimental procedures were meticulously executed in accordance with the manufacturer's instructions. With a standard curve $R^2 > 0.99$, the concentrations of IL-17, TGF-β, and fibronectin (FN) in the samples were calculated.

Immunohistochemical Staining of Peritoneal Tissue for IL-17
Peritoneal specimens were immediately fixed in 4% paraformaldehyde, followed by sequential dehydration with increasing concentrations of ethanol (70%–100%). The tissues were subsequently cleared in xylene and embedded in paraffin blocks. Thin sections (3 μm) were prepared, deparaffinized, and rehydrated with descending ethanol gradients. Antigen retrieval was performed using heat induction in a citrate buffer solution under pressure for 5 minutes. Endogenous peroxidase activity was quenched using a peroxidase inhibitor (OriGene Tech) at 37 °C for 30 minutes. Prior to antibody incubation, nonspecific epitopes were blocked with 10% goat serum (37 °C, 30 min). Tissue sections were then probed overnight at 4 °C with a rabbit-derived anti-IL-17 primary antibody (1:100 dilution). Following extensive washing, HRP-conjugated secondary antibodies were applied (37 °C, 30 min). Antigen-antibody interactions were visualized using 3,3'-diaminobenzidine (DAB) as a chromogen, and nuclear counterstaining was performed with Mayer's haematoxylin. Digital micrographs were acquired using a Leica DM6B brightfield microscope under standardized lighting conditions.

Real-time Quantitative PCR (RT-qPCR)
Total RNA was extracted from mouse peritoneal tissues using a column-based purification method. Before extraction, surgical instruments (forceps and scissors) and grinding beads were disinfected in 75% ethanol and dried in an oven at 60 °C for 15 minutes to ensure an RNase-free environment.
Approximately 30–50 mg of peritoneal tissue was placed into an RNase-free EP tube containing 500 μL of lysis buffer (Buffer RL) and two grinding beads. Tissues were homogenized for 5 minutes using a tissue grinder to ensure complete lysis. The homogenate was incubated at room temperature for 5 minutes and then centrifuged at 14,000×g for 5 minutes. The supernatant was transferred to a gDNA-depletion column to remove genomic DNA (14,000×g, 2 min). The flow-through was loaded onto an RNA purification column and washed sequentially with Buffer RW1 and ethanol-diluted Buffer RW2. After discarding the final wash solution, the column was centrifuged at 12,000×g for 2 minutes to remove residual ethanol. Finally, 30 μL of RNase-free water was added to the center of the column membrane. After incubation at room temperature for 2 minutes, total RNA was eluted by centrifugation and stored at −80 °C.
The concentration and purity of the isolated RNA were determined using a spectrophotometer. Samples with an A260/A280 ratio between 1.8 and 2.1 were used for subsequent experiments. Reverse transcription was performed using a two-step protocol to synthesize cDNA. First, the RNA concentration of each sample was adjusted to ensure equal template input. Residual genomic DNA was removed using a gDNA remover at 42 °C for 2 minutes. Subsequently, Hifair® III SuperMix plus was added to the reaction mixture. Reverse transcription was performed in a thermal cycler using the following program: 25 °C for 5 min, 55 °C for 15 min, and 85 °C for 5 min. The resulting cDNA was stored at −20°C.Real-time PCR was performed using the QuantStudio 6 Flex Real-time PCR System. The PCR reaction mixture (20 μL total volume) consisted of 10 μL SYBR Green Master Mix, 0.4 μL each of forward and reverse primers, 7.2 μL of DEPC-treated water, and 2 μL of cDNA template. All procedures were performed on ice and protected from direct light. Thermal cycling conditions were as follows: Initial denaturation: 95 °C for 5 min;
PCR cycles (40 cycles): 95 °C for 10 s (denaturation) and 60 °C for 30 s (annealing and extension); Melting curve analysis: A default melting curve program was run immediately after the final cycle to verify the specificity of amplification products.
The relative mRNA expression levels of target genes were calculated using the $2^{-\Delta\Delta Ct}$ method, with GAPDH used as the internal reference gene for normalization. Statistical analysis and data visualization were performed using GraphPad Prism 10 software.
The overall process of this study is shown in Figure 1.

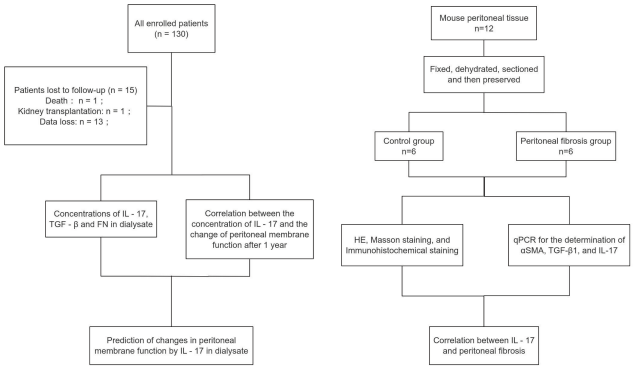

Figure 1. Flowchart of the overall study design.
This prospective cohort study enrolled 130 peritoneal dialysis (PD) patients. Peritoneal effluent samples were collected to measure IL-17, TGF-β, and fibronectin concentrations. Peritoneal function parameters were evaluated at baseline and after 1-year follow-up. A mouse model of peritoneal fibrosis (PF) was established to verify IL-17 expression in peritoneal tissues by immunohistochemistry and qPCR. Statistical analyses were performed to explore the association between effluent IL-17 and peritoneal solute transport rate (PSTR) decline.

Statistical Analysis
The collected and experimentally obtained data were analysed and organized. Continuous variables demonstrating a Gaussian distribution are presented as arithmetic means with

standard deviations (means ± SDs), whereas parameters violating normality assumptions are presented as median values accompanied by interquartile ranges (IQRs). When variable relationships between indicators followed a normal distribution and satisfied the assumptions of homogeneity of variance and independence, Pearson correlation analysis was applied; otherwise, Spearman correlation analysis was used. We implemented univariate and multivariate linear regression models to assess the predictive variables affecting ΔD/P Cr. In addition, we used binary logistic regression to analyse the interaction effect between IL-17 concentration and PD vintage on the binary outcome of increased PSTR (ΔD/P Cr > 0). We utilized Receiver operating characteristic (ROC) analysis to evaluate the prognostic capability of IL-17 for ΔD/P Cr > 0. Two-tailed tests were performed with α = 0.05, and the results were significant at the 0.05 level. All statistical analyses were performed with SPSS, GraphPad Prism, and R software.

Results

Baseline Characteristics

The study population comprised 130 patients receiving PD. All participants were included in the baseline characteristic analysis. As detailed in Table 1, 42.31% of the initial cohort were male, with a median age of 54 years (IQR 44.25–60.00). The mean BMI was 23.10 ± 3.14 kg/m². At baseline, the median peritoneal effluent IL-17 concentration was 40.49 pg/mL (IQR 39.00–41.79 pg/mL). For peritoneal transport parameters, the mean baseline D/P Cr was 0.62 ± 0.10, and the median baseline D/D0 glucose was 0.42 (IQR 0.36–0.47). After 1 year of follow-up, 15 patients were censored (due to death, transplantation, or loss to follow-up), leaving 115 patients (88.5%) for the final outcome analysis. The baseline characteristics of the analyzed cohort (N = 115) are also presented in Table 1 (second column) and were comparable to the initial cohort (all P > 0.05), indicating no significant selection bias. Detailed comparisons are provided in Supplementary Table 1.

Participants were dichotomized based on PSTR into a non-increased PSTR group (Group A: ΔD/P Cr ≤ 0, n = 50) and an increased PSTR group (Group B: ΔD/P Cr > 0, n = 65). Statistical analysis revealed that baseline D/P Cr (Figure 2A, P = 0.001), D/D0 glucose (P = 0.002), peritoneal creatinine clearance (pCcr) (P = 0.013), and IL-17 concentration (Figure 2B, P < 0.0001) differed significantly between the two groups, whereas PD vintage (Figure 2C) and other parameters showed no significant differences.

Correlation between Effluent IL-17 and Changes in PSTR

To quantitatively assess the correlation between cytokines and profibrotic factors, the associations between effluent IL-17 and both TGF-β and FN were calculated. Correlation analysis revealed a marked positive correlation between IL-17 and both TGF-β (r = 0.440, P < 0.001) and FN (r = 0.319, P < 0.01). The scatter plot distributions illustrating these linear associations are depicted in Figure 2D and 2E. Furthermore, the positive correlation between IL-17 and ΔD/P Cr (r = 0.318, P < 0.01) suggests the clinical application value of IL-17 (Figure 2F).

Predictive Value of IL-17 for Peritoneal Transport Status

To identify the vital predictors of PSTR, we constructed univariate and multivariate regression models (Table 2). Univariate analysis revealed that only baseline D/P Cr was independent predictor of D/P Cr one year later. However, in the multivariable regression analysis incorporating PD vintage, age, CRP, baseline D/P Cr, pCcr and IL-17 as covariates, baseline D/P Cr (β = 0.791, P < 0.001) and IL-17 (β = 0.006, P = 0.022) were identified as independent predictors of D/P Cr one year later. In the multivariate model, after adjustment for other variables, each 1 pg/mL increase in effluent IL-17 concentration predicted an average increase of 0.006 units in 1-year D/P Cr. Similarly, each 1-unit increase in baseline D/P Cr was associated with an average increase of 0.791 units in 1-year D/P Cr.

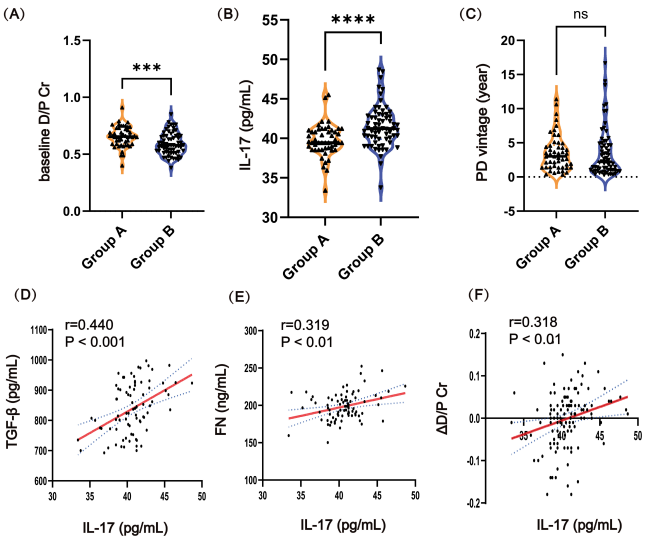

Figure 2. Comparisons of baseline indicators and correlation analysis of IL-17.

(**A**) Comparison of baseline dialysate-to-plasma creatinine ratio (D/P Cr) between non-increased PSTR group (Group A) and increased PSTR group (Group B). (**B**) Comparison of peritoneal effluent IL-17 levels between two groups. (**C**) Comparison of PD vintage between two groups. (**D**) Correlation between effluent IL-17 and TGF-β. (**E**) Correlation between effluent IL-17 and fibronectin (FN). (**F**) Correlation between effluent IL-17 and ΔD/P Cr.

Note: ***P < 0.001, ****P < 0.0001

To further investigate the predictive value of IL-17 for changes in peritoneal function, we evaluated its association with 1-year D/D0 glucose (Table 3). Univariate analysis identified baseline D/P Cr, baseline D/D0 glucose, and pCcr as significant correlates of 1-year D/D0 glucose. However, after adjustment for baseline peritoneal function parameters, only baseline D/D0 glucose (β = 0.474, P < 0.001) and IL-17 (β = −0.005, P = 0.040) remained independent predictors of 1-year D/D0 glucose.

We constructed a binary logistic regression model to assess the joint effect of IL-17 levels and PD vintage on an increased PSTR. To explore this interaction, an interaction term (IL-17 × PD vintage) was included in the model. Notably, PD vintage significantly modified the association between IL-17 and peritoneal transport status (P for interaction = 0.028). As shown in Figure 3A, the predictive effect of IL-17 on faster PSTR was weaker in the short-term dialysis group (1 year). However, this association became significantly stronger in patients with longer dialysis durations (3 and 5 years). The increasingly steep

https://doi.org/10.71321/g94y8w65

Table 1. Baseline Characteristics of the Overall Study Population and Patients Who Completed Follow-up.

Index	Total (n=130)	Follow-up (n=115)		t/Z/X²	P value
		Group A (n=50)	Group B (n=65)		
Gender				0.416	0.519
Male (%)	55 (42.31%)	23 (46.00%)	26 (40.00%)		
Female (%)	75 (57.69%)	27 (54.00%)	39 (60.00%)		
Hypertension				1.410	0.235
No	29 (22.31%)	13 (26.00%)	11 (16.92%)		
Yes	101 (77.69%)	37 (74.00%)	54 (83.08%)		
Diabetes				1.441	0.230
No	114 (87.69%)	46 (92.00%)	55 (84.62%)		
Yes	16 (12.31%)	4 (8.00%)	10 (15.38%)		
age (year)	54.00 (44.25, 60.00)	52 (40.5,59)	54 (49,60)	-1.115	0.265
BMI (kg/m²)	23.10 ± 3.14	23.17 (20.88,25.03)	22.86 (20.44,25.75)	-0.166	0.868
PD vintage (year)	2.60 (1.21, 4.71)	3.01 (1.4,4.66)	2.23 (0.97,4.94)	-0.852	0.394
baseline D/P Cr	0.62 ± 0.10	0.65±0.09	0.59±0.1	3.579	<0.001***
baseline D/D0 Glucose	0.42 (0.36, 0.47)	0.39±0.08	0.44±0.08	-3.184	0.002**
Urea kinetics					
Peritoneal Kt/V	1.54 ± 0.47	1.6±0.51	1.52±0.43	0.846	0.399
Renal Kt/V	0.14 (0, 0.6)	0.08 (0,0.46)	0.21 (0,0.66)	-0.953	0.341
Total Kt/V	1.87 ± 0.52	1.88±0.59	1.9±0.48	-0.269	0.789
Creatinine clearance (L/wk/1.73 m²)					
pCcr	38.79±8.95	41.41±9.04	37.11±9	2.534	0.013*
rCcr	4.38 (0,26.12)	2.18 (0,14.23)	9.1 (0,28.69)	-1.268	0.205
Total Ccr	50.13 (42.88,61.76)	50.52 (43.09,57.51)	50.24 (41.77,62.89)	-0.195	0.846
SCr (umol/L)	959.66±271.67	990.06±274.29	949.87±279.93	0.770	0.443
BUN (mmol/L)	20.16±5.54	20.3±5.43	20.02±5.51	0.275	0.784
PTH (pg/mL)	277 (120.75, 397)	289.5 (182.25,412.25)	261 (125.5,379.5)	-1.162	0.245
Hb (g/L)	109.71 ± 20.31	106.36±17.93	109.88±20.78	-0.954	0.342
ALB (g/L)	37.85 ± 3.87	37.48±4.12	38.36±3.49	-1.237	0.219
TG (mmol/L)	1.53 (1.07, 2.48)	1.42 (1.03,2.42)	1.9 (1.19,2.9)	-1.704	0.088
TC (mmol/L)	4.76 ± 1.32	4.61±1.08	4.83±1.43	-0.902	0.369
Glucose (mmol/L)	4.87 (4.3, 5.72)	4.84 (4.2,5.49)	4.97 (4.42,6.09)	-0.886	0.376
Corrected calcium (mmol/L)	2.35 (2.21, 2.45)	2.36 (2.21,2.47)	2.34 (2.18,2.44)	-0.753	0.451
P (mmol/L)	1.80 ± 0.47	1.78±0.47	1.85±0.47	-0.889	0.376
Ca×P product	4.10 (3.28, 4.84)	3.97 (3.43,4.53)	4.31 (3.22,5.08)	-0.739	0.460
NE (x10 ^{9} /L)	4.19 (3.34, 5.4)	4.05 (3.47,5.17)	4.27 (3.3,5.54)	-0.553	0.580
LYM (x10 ^{9} /L)	1.32 (1.1, 1.65)	1.26 (1.03,1.6)	1.41 (1.14,1.73)	-1.786	0.074
MONO (x10 ^{9} /L)	0.41 (0.31, 0.54)	0.43 (0.29,0.55)	0.41 (0.32,0.55)	-0.186	0.852
PLT (x10 ^{9} /L)	197.62 ± 66.19	195 (144.25,228.5)	190 (167.5,249)	-0.920	0.358
CRP (mg/L)	1.63 (0.6, 3.59)	1.24 (0.39,2.63)	1.79 (0.73,3.86)	-1.334	0.182
EF (%)	62 (60, 65.25)	62 (60,66)	63 (60,66)	-0.368	0.713
LA (cm)	3.70 ± 0.49	3.76 (3.32,4.22)	3.55 (3.35,4.05)	-0.866	0.386
LVD (cm)	4.77 (4.33, 5.06)	4.72 (4.38,5.06)	4.8 (4.33,5.07)	-0.316	0.752
LVPWD (cm)	0.95 (0.89, 1.04)	0.98 (0.9,1.07)	0.94 (0.88,1.03)	-1.672	0.094
D/P Cr 1 year later	-	0.59 (0.54,0.65)	0.61 (0.57,0.71)	-2.047	0.041*
D/D0 Glucose 1 year later	-	0.44 (0.41,0.50)	0.44 (0.36,0.47)	-1.534	0.125
IL-17 (pg/mL)	40.49 (39, 41.79)	39.45 (38.55,41.04)	41.25 (39.9,42.9)	-3.858	<0.0001****

Note: Group A: non-increased PSTR group; Group B: increased PSTR group. Normally distributed continuous variables are expressed as mean ± standard deviation (mean ± SD); non-normally distributed continuous variables are expressed as median (interquartile range) [M (P25, P75)]; categorical variables are expressed as number (%). *P < 0.05; **P < 0.01; ***P < 0.001; ****P < 0.0001.

slopes indicate that the deleterious effect of elevated IL-17 on faster PSTR is exacerbated by prolonged PD exposure.

Incremental Predictive Value of IL-17 over Standard Clinical Metrics

While the standard clinical model (including baseline D/P Cr and pCcr) showed acceptable accuracy in predicting faster PSTR (ΔD/P Cr > 0) (the area under the curve [AUC] = 0.705, 95% CI: [0.609–0.801]), the addition of effluent IL-17 significantly enhanced the accuracy. Specifically, the comprehensive model (IL-17 + baseline D/P Cr + pCcr) achieved the optimal predictive accuracy, with an AUC of 0.789 (95% CI: 0.706–0.872), a sensitivity of 72.3%, and a specificity of 74.0%. DeLong test confirmed that this comprehensive model was statistically superior to the base model (P < 0.05; Figure 3B and Table 4). These findings highlight the incremental predictive value of IL-17, indicating that it captures changes in peritoneal function that cannot be reflected by baseline transport status.

Validation of IL-17 Expression in A Mouse Peritoneal Fibrosis Model

To investigate the specific role of IL-17 in the pathogenesis of peritoneal fibrosis in vivo, we established a murine PF model by daily intraperitoneal injection of 4.25% glucose-based dialysis fluid. As shown in Figure 4A, haematoxylin and eosin (HE) staining revealed notable thickening of the peritoneum and increased inflammatory cell infiltration in the fibrosis group compared with the control group. Masson staining showed that collagen deposition was significantly increased in fibrotic peritoneal tissue. Moreover, immunohistochemistry (IHC) demonstrated marked infiltration of IL-17-positive cells within the fibrotic tissues. These results verified the successful induction of the PF model and indicated that IL-17 expression was upregulated in the fibrotic peritoneum.

qPCR Assessment of Fibrotic Markers and IL-17 mRNA Expression in Murine Peritoneal Tissue

To further quantify the extent of peritoneal injury and inflammatory status at the molecular level, real-time quantitative PCR (qPCR) was employed to determine the mRNA expression

Table 2. Univariable and Multivariable Linear Regression of Influencing Factors on D/P Cr.

Variables	Univariate Analysis		Multivariate Analysis	
	β(95%CI)	P-value	β (95%CI)	P-value
PD vintage (years)	0.003 (-0.003, 0.009)	0.284	0.001 (-0.004, 0.005)	0.820
Age(years)	0.001 (-0.0002, 0.003)	0.084	0.001 (0.000, 0.002)	0.205
CRP(mg/L)	0.002 (-0.004, 0.007)	0.499	0.0003 (-0.003, 0.004)	0.853
ALB (g/L)	-0.008 (-0.012, -0.003)	0.001**	0.0002 (-0.003, 0.004)	0.927
Baseline D/P Cr	0.742 (0.623, 0.861)	<0.001***	0.791 (0.648, 0.934)	< 0.001***
pCcr	0.003 (0.001, 0.005)	0.002**	-0.001 (-0.003, 0.001)	0.248
IL-17(pg/mL)	0.003 (-0.004, 0.010)	0.411	0.006 (0.001, 0.011)	0.022*

Note: *P < 0.05, **P < 0.01, ***P < 0.001.

Table 3. Univariable and Multivariable Linear Regression of Influencing Factors on D/D 0 glucose.

Variables	Univariate Analysis		Multivariate Analysis	
	β(95%CI)	P-value	β (95%CI)	P-value
PD vintage (years)	-0.004 (-0.008, 0.001)	0.129	-0.002 (-0.006, 0.002)	0.307
ALB (g/L)	0.005 (0.001, 0.008)	0.017*	0.0001 (-0.003, 0.003)	0.946
Baseline D/P Cr	-0.473 (-0.594, -0.352)	<0.001***	-0.166 (-0.370, 0.039)	0.111
Baseline D/D0 Glucose	0.626 (0.484, 0.768)	<0.001***	0.474 (0.238, 0.711)	<0.001***
peritoneal Kt/V	0.020 (-0.011, 0.052)	0.207	0.031 (0.005, 0.057)	0.022*
pCcr	-0.002 (-0.004, -0.001)	0.002**	0.000 (-0.002, 0.002)	0.922
IL-17(pg/mL)	-0.003 (-0.009, 0.003)	0.282	-0.005 (-0.010, -0.0002)	0.040*

Note: *P < 0.05, **P < 0.01, ***P < 0.001.

Table 4. Comparison of ROC Curve Parameters for Prediction Models of faster PSTR.

	Groups	AUC	95%CI	Optimal Cutoff	Sensitivity (%)	Specificity (%)
Model 1	IL-17	0.710	0.617-0.804	39.86	76.9	58.0
Model 2	baseline D/P Cr	0.694	0.597-0.790	0.605	63.1	72.0
Model 3	pCcr	0.633	0.529-0.737	37.88	53.8	72.0
Model 4	baseline D/P Cr + pCcr	0.705	0.609-0.801	-	84.6	50.0
Model 5	baseline D/P Cr + pCcr+ IL-17	0.789	0.706-0.872	-	72.3	74.0

levels of fibrotic markers (α-SMA and TGF-β) and IL-17 in the experimental groups. As shown in Figure 4B-D, mRNA expression of α-SMA in peritoneal tissues was significantly higher in the PF group than in the control group ($P < 0.05$). Similarly, the mRNA levels of TGF-β in the PF group were significantly higher than those in the control group ($P < 0.01$). Furthermore, IL-17 mRNA expression in the PF group showed a marked upregulation compared with the control group ($P < 0.05$). These transcriptional findings were consistent with the previously observed trend in IL-17 protein expression as determined by immunohistochemical staining.

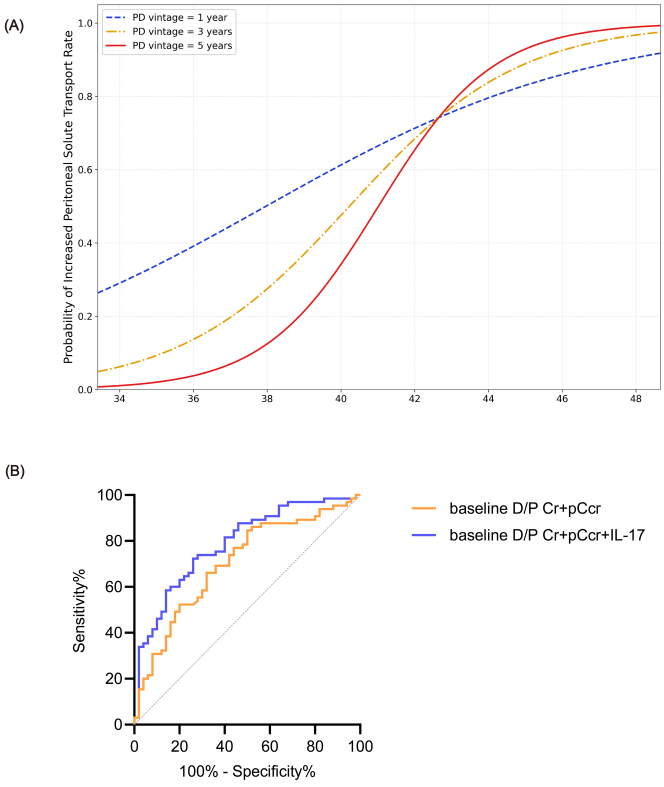

Figure 3. Interaction effect and receiver operating characteristic (ROC) curve analysis.

(**A**) Predicted probability plot showing the interaction between IL-17 concentration and PD vintage on faster PSTR. (**B**) ROC curves of baseline model (D/P Cr + pCcr) and combined model (D/P Cr + pCcr + IL-17) for predicting faster PSTR.

Discussion

This study represents the first prospective cohort analysis to establish that effluent IL-17 serves as a reliable predictor of faster PSTR. There is a statistically significant correlation between elevated PSTR and increased mortality rate, as well as a trend toward a higher technical failure rate [18-19]. However, traditional clinical criteria still lack the sensitivity required for early monitoring of PSTR increase. Our study bridges this gap and reveals that compared with the standard clinical model, the model incorporating IL-17 has significant predictive value. Additionally, the histological evidence from the mouse peritoneal fibrosis model further supports the feasibility of using IL-17 as an early biomarker for peritoneal fibrosis.

Univariate regression analysis demonstrated that baseline D/P Cr was the most robust predictor of peritoneal transport status at the 1-year follow-up ($\beta = 0.742$, $P < 0.001$). This finding underscores the inherent stability of peritoneal membrane characteristics, where initial solute transport rates—likely reflecting baseline microvascular density and anatomical integrity—largely dictate subsequent functional trajectories. Consequently, adjusting for initial functional status is imperative when isolating the contributions of auxiliary pathogenic factors. Notably, after adjusting for baseline D/P Cr and systemic inflammatory markers (CRP and albumin), local peritoneal IL-17 levels remained independently associated with the progression of D/P Cr ($\beta = 0.006$, $P = 0.022$). These data suggest that IL-17-mediated local immune-inflammatory responses may serve as an independent driver of peritoneal transport acceleration. Even in the absence of systemic inflammation, elevated intraperitoneal IL-17 may herald a shift toward a high-transporter phenotype within the following year.

In an experimental fibrosis model induced by glucose-rich dialysis fluid, significant peritoneal thickening, abnormal collagen deposition, and increased IL-17 expression were observed. These morphological changes were consistent with the findings of González-Mateo et al. and Ferrantelli et al., who explained that IL-17 blockade attenuated peritoneal fibrosis [20-21], further confirming the role of IL-17 in peritoneal structural deterioration. This profibrotic potential was further supported by in vivo evidence. These pathological alterations impair peritoneal function, especially by affecting solute transport and

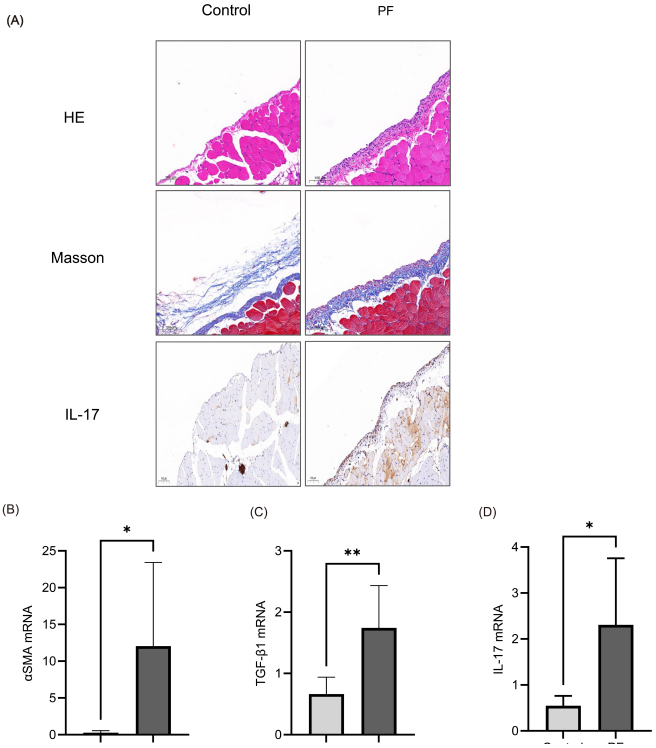

Figure 4. Histological staining and mRNA expression in mouse peritoneal tissues.

(**A**) Representative images of HE staining, Masson staining, and IL-17 immunohistochemical staining in peritoneal tissues from control and PF mice (scale bar = 100 μm, 100× magnification). Relative mRNA expression of (**B**) α-SMA mRNA, (**C**) TGF-β1 mRNA, and (**D**) IL-17 mRNA in peritoneal tissues. *$P < 0.05$, **$P < 0.01$.

ultrafiltration, ultimately resulting in dialysis technique failure [22]. Previous studies have indicated that bioincompatible dialysis fluids induce Th17 polarization and IL-17 secretion [23]. This process activates mesothelial cells, prompting the release of proinflammatory mediators that modulate the local inflammatory microenvironment. This cascade initiates and amplifies peritoneal damage, laying the pathological foundation for the progression of fibrosis. Local peritoneal microinflammation, which intensifies with increasing PD vintage, serves as a pivotal factor driving structural remodelling, including fibrosis, vascular lesions, and abnormal lymphatic vessel formation [24].

Our data also revealed robust positive correlations between effluent IL-17 and both TGF-β (r = 0.440) and FN (r = 0.319). TGF-β is a well- recognized promoter of mesothelial-to-mesenchymal transition (MMT), and FN drives extracellular matrix (ECM) remodelling [25-26]. Mechanistically, we hypothesize that these associations stem from a pathogenic positive feedback loop in which IL-17 upregulates TGF-β expression [26]. In accordance with previous findings, IL-17 activates the ERK and TGF-β/Smad pathways to drive ECM production [16, 27]. Simultaneously, TGF-β enhances the inflammatory response by inducing Th17 polarization. This interaction accelerates the transition from chronic inflammation to irreversible fibrosis. This irreversible pathological damage results in a significant reduction in peritoneal capacity, ultimately compromises the clinical success of dialysis. Such pathological change in peritoneal structure can only be diagnosed via peritoneal biopsy. However, its clinical application is limited due to the invasive nature of the procedure. Clinically, the results of PET are used to assess the function of the peritoneum.

Moreover, our research demonstrates that the comprehensive model incorporating IL-17 has greater predictive value than the basic model that includes only baseline D/P Cr and pCcr. ROC analysis confirmed this enhanced efficacy, and the results were validated by the DeLong test ($P < 0.05$). These findings suggest that the effluent IL-17 has independent clinical prognostic value. Furthermore, our logistic regression model revealed a statistically significant interaction between IL-17 levels and PD duration ($P = 0.028$). As shown in Figure 3A, higher effluent IL-17 levels predicted an increased risk of faster PSTR, and this association was more pronounced in patients with long-term PD. Conversely, no such trend was observed in the short-term treatment group. These results suggest that the prognostic discriminatory ability of IL-17 strengthens with increasing dialysis vintage.

These observations align with those of Poniewierska-Baran et al. [15] and Shao et al. [28], supporting the hypothesis that prolonged exposure to bioincompatible dialysis fluids continuously activates Th17 cells. As a well-recognized inflammatory factor, IL-17 was found to be significantly positively correlated with serum CRP levels and PD vintage. This positive correlation is in accordance with the hypothesis that a chronic inflammatory response occurs in the peritoneum of PD patients. Additionally, the positive relationship between IL-17 levels and corrected serum calcium levels suggests that IL-17 may be involved in calcium and phosphorus metabolism disorders. Consequently, IL-17 acts as an important time-varying factor within the peritoneal microenvironment. For patients with a long dialysis duration, close monitoring of IL-17 levels is essential for timely clinical intervention.

This study has the following limitations: the single-centre study design may limit its generalizability. Although the 12-month follow-up confirmed the predictive value of IL-17, it may not fully capture long-term structural outcomes.

Conclusion

In conclusion, this study demonstrated that IL-17 in the effluent serves as a potent biomarker for predicting faster PSTR. By elucidating the synergistic role of IL-17 in peritoneal fibrosis, our findings reveal a candidate biomarker for early detection and clinical intervention. Identifying high-risk populations enables the timely adjustment of treatment regimens, ultimately offering a strategy to optimize survival prospects within the PD population.

Abbreviations

4 h UF - 4-hour ultrafiltration volume; Alb - Albumin; AUC - Area Under the Curve; BMI - Body mass index; BUN - Blood urea nitrogen; CA125 - Cancer antigen 125; CRP - C-reactive protein; D/D0 glucose - Dialysate-to-initial dialysate glucose ratio; D/P Cr - Dialysate-to-plasma creatinine ratio; EF - Ejection fraction; ELISA - Enzyme-linked immunosorbent assay; ESRD - End-stage renal disease; FN - Fibronectin; Hb - Haemoglobin; IHC - Immunohistochemistry; IL-17 - Interleukin-17; IL-6 - Interleukin-6; LA - Left atrial diameter; LVD - Left ventricular diameter; LVPWD - Left ventricular posterior wall thickness; LYM - Lymphocyte count; MMT - Mesothelial-to-mesenchymal transition; MONO - Monocyte count; NE - Neutrophil count; NF-κB - Nuclear factor kappa-B; pCcr - Peritoneal creatinine clearance; PD - Peritoneal Dialysis; PET - Peritoneal equilibration test; PF - Peritoneal Fibrosis; PSTR - Peritoneal solute transport rate; PTH - Parathyroid hormone; rCcr - Renal creatinine clearance; ROC - Receiver Operating Characteristic; RORγt - Retinoic acid-related orphan receptor gamma t; RT-qPCR - Real-time Quantitative PCR; SCr - Serum creatinine; TC - Total cholesterol; TG - Triglyceride; TGF-β - Transforming growth factor β; Th17 - T helper 17; UFF - Ultrafiltration failure.

Author Contributions

Lejia Song: Conceptualization, Methodology, Investigation, Formal analysis, Writing-original draft. Lu Li: Methodology, Supervision, Resources. Guang Chen: Validation, Software. Qiufeng Wang: Resources, Data curation. Qingqing Rao: Supervision, Investigation. Huaina Dou: Formal Analysis, Visualization. Li Zhang: Investigation,Software. Pei Zhang (Corresponding Author): Conceptualization, Funding Acquisition, Supervision, Validation, Writing-Review & Editing; All authors read and approved the final manuscript.

Acknowledgements

We would like to thank all the patients who participated in this study and the medical staff at the Department of Nephrology, the First Affiliated Hospital of Anhui Medical University, for

their assistance in data collection and patient follow-up.

Funding Information

This work was supported by the Anhui Provincial Natural Science Foundation (Grant No. 2408085MH208).

Ethics Approval and Consent to Participate

The studies involving human participants were reviewed and approved by the Ethics Committee of the First Affiliated Hospital of Anhui Medical University (Approval No. PJ 2025-08-97). The animal study protocol was approved by the Animal Ethics Committee of Anhui Medical University (Approval Number: LLSC20241406). The human study was conducted in accordance with the Declaration of Helsinki (as revised in 2013).

Competing Interests

The authors declare that they have no known competing financial interests or personal relationships that could have appeared to influence the work reported in this paper.

Data Availability

The data that support the findings of this study are available from the corresponding author upon reasonable request. The data are not publicly available due to privacy or ethical restrictions.

References

[1] Cho Y, Bello AK, Levin A, Lunney M, Osman MA, Ye F, et al. (2021). Peritoneal Dialysis Use and Practice Patterns: An International Survey Study. Am J Kidney Dis, 77(3), 315–325. https://doi.org/10.1053/j.ajkd.2020.05.032

[2] Suryantoro SD, Thaha M, Sutanto H, & Firdausa S. (2023). Current Insights into Cellular Determinants of Peritoneal Fibrosis in Peritoneal Dialysis: A Narrative Review. J Clin Med, 12(13). https://doi.org/10.3390/jcm12134401

[3] Teitelbaum I. (2021). Peritoneal Dialysis. N Engl J Med, 385(19), 1786–1795. https://doi.org/10.1056/NEJMra2100152

[4] Gu J, Bai E, Ge C, Winograd J, & Shah AD. (2023). Peritoneal equilibration testing: Your questions answered. Perit Dial Int, 43(5), 361–373. https://doi.org/10.1177/08968608221133629

[5] Brimble KS, Walker M, Margetts PJ, Kundhal KK, & Rabbat CG. (2006). Meta-analysis: peritoneal membrane transport, mortality, and technique failure in peritoneal dialysis. J Am Soc Nephrol, 17(9), 2591–2598. https://doi.org/10.1681/asn.2006030194

[6] Mehrotra R, Ravel V, Streja E, Kuttykrishnan S, Adams SV, Katz R, et al. (2015). Peritoneal Equilibration Test and Patient Outcomes. Clin J Am Soc Nephrol, 10(11), 1990–2001. https://doi.org/10.2215/cjn.03470315

[7] Graterol Torres F, Molina M, Soler-Majoral J, Romero-González G, Rodríguez Chitiva N, Troya-Saborido M, et al. (2022). Evolving concepts on inflammatory biomarkers and malnutrition in chronic kidney disease. Nutrients, 14, 4297. https://doi.org/10.3390/nu14204297

[8] Prasad N, Chaturvedi S, Singh H, Udumula MP, Rawat A, Jeyakumar M, et al. (2025). Peritoneal Dialysis -Associated Fibrosis: Emerging Mechanisms and Therapeutic Opportunities. Front Pharmacol, 16, 1635624. https://doi.org/10.3389/fphar.2025.1635624

[9] Iwakura Y, Ishigame H, Saijo S, & Nakae S. (2011). Functional specialization of interleukin-17 family members. Immunity, 34(2), 149–162. https://doi.org/10.1016/j.immuni.2011.02.012

[10] Marchant V, Tejera-Muñoz A, Marquez-Expósito L, Rayego-Mateos S, Rodrigues-Diez RR, Tejedor L, et al. (2020). IL-17A as a Potential Therapeutic Target for Patients on Peritoneal Dialysis. Biomolecules, 10(10). https://doi.org/10.3390/biom10101361

[11] Witowski J, Kamhieh-Milz J, Kawka E, Catar R, & Jörres A. (2018). IL-17 in Peritoneal Dialysis-Associated Inflammation and Angiogenesis: Conclusions and Perspectives. Front Physiol, 9, 1694. https://doi.org/10.3389/fphys.2018.01694

[12] Rodrigues-Díez R, Aroeira LS, Orejudo M, Bajo MA, Heffernan JJ, Rodrigues-Díez RR, et al. (2014). IL-17A is a novel player in dialysis-induced peritoneal damage. Kidney Int, 86(2), 303–315. https://doi.org/10.1038/ki.2014.33

[13] Huang L. (2024). The role of IL-17 family cytokines in cardiac fibrosis. Front Cardiovasc Med, 11, 1470362. https://doi.org/10.3389/fcvm.2024.1470362

[14] Xiao H, Peng L, Jiang D, Liu Y, Zhu L, Li Z, et al. (2022). IL-17A promotes lung fibrosis through impairing mitochondrial homeostasis in type II alveolar epithelial cells. J Cell Mol Med, 26(22), 5728–5741. https://doi.org/10.1111/jcmm.17600

[15] Poniewierska-Baran A, Tabarkiewicz J, Radzikowska U, Tynecka M, & Eljaszewicz A. (2024). The pivotal role of IL-17A in hepatic stellate cell activation. Cent Eur J Immunol, 49(4), 331. https://doi.org/10.5114/ceji.2024.146900

[16] Liu F, Wang J, Sun Z, & Yu X. (2025). Rehmannioside A alleviates renal inflammation and fibrosis in hypertensive nephropathy via AT1R/MAPK14/IL-17 signaling pathway. Biochem Biophys Res Commun, 776, 152237. https://doi.org/10.1016/j.bbrc.2025.152237

[17] Zhou YN, Xia JK, Shi CR, He Y, & Shang SL. (2025). Crosstalk Between Th17 Cells and Renal Tubular Epithelial Cells Promotes Fibrotic Progression in IgA Nephropathy. Curr Med Sci, 45(3), 626–639. https://doi.org/10.1007/s11596-025-00068-6

[18] Chung SH, Heimbürger O, & Lindholm B. (2008). Poor outcomes for fast transporters on PD: the rise and fall of a clinical concern. Semin Dial, 21(1), 7–10. https://doi.org/10.1111/j.1525-139X.2007.00327.x

[19] Huang G, Wang Y, Shi Y, Ma X, Tao M, Zang X, et al. (2021). The prognosis and risk factors of baseline high peritoneal transporters on patients with peritoneal dialysis. J Cell Mol Med, 25(18), 8628–8644. https://doi.org/10.1111/jcmm.16819

[20] González-Mateo GT, Fernández-Míllara V, Bellón T, Liappas

G, Ruiz-Ortega M, López-Cabrera M, et al. (2014). Paricalcitol reduces peritoneal fibrosis in mice through the activation of regulatory T cells and reduction in IL-17 production. PLoS One, 9(10), e108477. https://doi.org/10.1371/journal.pone.0108477

[21] Ferrantelli E, Liappas G, Vila Cuenca M, Keuning ED, Foster TL, Vervloet MG, et al. (2016). The dipeptide alanyl-glutamine ameliorates peritoneal fibrosis and attenuates IL-17 dependent pathways during peritoneal dialysis. Kidney Int, 89(3), 625–635. https://doi.org/10.1016/j.kint.2015.12.005

[22] Ito Y, Sun T, Tawada M, Kinashi H, Yamaguchi M, Katsuno T, et al. (2024). Pathophysiological Mechanisms of Peritoneal Fibrosis and Peritoneal Membrane Dysfunction in Peritoneal Dialysis. Int J Mol Sci, 25(16). https://doi.org/10.3390/ijms25168607

[23] Helmke A, Hüsing AM, Gaedcke S, Brauns N, Balzer MS, Reinhardt M, et al. (2021). Peritoneal dialysate-range hypertonic glucose promotes T-cell IL-17 production that induces mesothelial inflammation. Eur J Immunol, 51(2), 354–367. https://doi.org/10.1002/eji.202048733

[24] Li XR, Yang SK, Zeng BY, Tian J, Liu W, & Liao XC. (2023). Relationship between peritoneal solute transport and dialysate inflammatory markers in peritoneal dialysis patients: A cross-sectional study. Nefrologia (Engl Ed), 43(3), 335–343. https://doi.org/10.1016/j.nefroe.2022.12.001

[25] Huang Q, Xiao R, Lu J, Zhang Y, Xu L, Gao J, et al. (2022). Endoglin aggravates peritoneal fibrosis by regulating the activation of TGF-β/ALK/Smads signaling. Front Pharmacol, 13, 973182. https://doi.org/10.3389/fphar.2022.973182

[26] Lurje I, Gaisa NT, Weiskirchen R, & Tacke F. (2023). Mechanisms of organ fibrosis: Emerging concepts and implications for novel treatment strategies. Mol Aspects Med, 92, 101191. https://doi.org/10.1016/j.mam.2023.101191

[27] Zhang Y, Feng W, Peng X, Zhu L, Wang Z, Shen H, et al. (2022). Parthenolide alleviates peritoneal fibrosis by inhibiting inflammation via the NF-κB/ TGF-β/Smad signaling axis. Lab Invest, 102(12), 1346–1354. https://doi.org/10.1038/s41374-022-00834-3

[28] Shao X, Yao L, Fu J, He M, & Zhang P. (2024). Differential expression and clinical significance of IGF2BP3 in peritoneal dialysate of patients with varying duration of peritoneal dialysis. Clin Transl Sci, 17(4), e13774. https://doi.org/10.1111/cts.13774